

# Gd<sub>2</sub>O(CO<sub>3</sub>)<sub>2</sub>·H<sub>2</sub>O Particles and the Corresponding Gd<sub>2</sub>O<sub>3</sub>: Synthesis and Applications of Magnetic Resonance Contrast Agents and Template Particles for Hollow Spheres and Hybrid Composites

The solution approach was employed to yield multifunctional amorphous Gd<sub>2</sub>O(CO<sub>3</sub>)<sub>2</sub>·H<sub>2</sub>O colloidal spheres by a reflux of an aqueous solution containing GdCl<sub>3</sub>·6H<sub>2</sub>O and urea. By elongating the reaction time, crystalline rhombus-shaped Gd<sub>2</sub>O(CO<sub>3</sub>)<sub>2</sub>·H<sub>2</sub>O with at least 87% yield could be formed. High-resolution synchrotron powder X-ray diffraction provides crystal structure information, such as cell dimensions, which indexes the exact crystal packing with hexagonal symmetry, for the crystalline rhombus sample. Particle formation was studied based on the reaction time and the concentration ratio of [urea]/[GdCl<sub>3</sub>·6H<sub>2</sub>O]. After a calcination process, the amorphous spheres and crystalline rhombus Gd<sub>2</sub>O(CO<sub>3</sub>)<sub>2</sub>·H<sub>2</sub>O particles convert into crystalline Gd<sub>2</sub>O<sub>3</sub> at temperatures above 600 °C. For *in vitro* magnetic resonance imaging (MRI), both Gd<sub>2</sub>O(CO<sub>3</sub>)<sub>2</sub>·H<sub>2</sub>O and Gd<sub>2</sub>O<sub>3</sub> species show the promising T<sub>1</sub>- and T<sub>2</sub>-weighted effects. The amorphous Gd<sub>2</sub>O(CO<sub>3</sub>)<sub>2</sub>·H<sub>2</sub>O contrast agent further demonstrates enhanced contrast of the liver and kidney using a dynamic contrast-enhanced MR imaging (DCE-MRI) technique for *in vivo* investigation. The multifunctional capability of the spheres was also evidenced by the formation of nanoshells. Surface engineering of the amorphous Gd<sub>2</sub>O(CO<sub>3</sub>)<sub>2</sub>·H<sub>2</sub>O spheres could be performed by covalent bonding to form hollow silica nanoshells and hollow silica@Fe<sub>3</sub>O<sub>4</sub> hybrid particles.

## ◎ Beamline

01C2 SWLS-X-ray Powder Diffraction

## ◎ Authors

**C.-S. Yeh and I.-F. Li**

National Cheng Kung University, Tainan, Taiwan

**C.-H. Su**

National Taiwan University, Taipei, Taiwan

**H.-S. Sheu**

National Synchrotron Radiation Research Center, Hsinchu, Taiwan



Recently, research has been centred on the fabrication of the multifunctional inorganic-based particulate agents for *in vitro* and *in vivo* biomedical applications. The non-invasive MRI, recognized as harmless to the body, provides anatomical details in diagnosis and offers highly resolved contrast. Currently, MR contrast agents are categorized into T<sub>1</sub>-positive agents of paramagnetic species, such as gadolinium (Gd<sup>3+</sup>)-based complexes and T<sub>2</sub>-negative agents of superparamagnetic iron oxide particles. Herein, we report the synthesis and applications of Gd<sub>2</sub>O(CO<sub>3</sub>)<sub>2</sub>·H<sub>2</sub>O colloidal particles and their corresponding Gd<sub>2</sub>O<sub>3</sub>. The Gd<sub>2</sub>O(CO<sub>3</sub>)<sub>2</sub>·H<sub>2</sub>O spherical particles exhibited multifunctional capability by the observation of showing MR contrast effect and developing as multimodal materials. Our findings can be categorized to three main themes: (i) We wish to present the first report of the Gd<sub>2</sub>O(CO<sub>3</sub>)<sub>2</sub>·H<sub>2</sub>O colloidal particles, which readily synthesized with GdCl<sub>3</sub>·6H<sub>2</sub>O and urea by reflux process under a low temperature. With the detailed characterization of the high resolution synchrotron powder X-ray diffraction, crystal structural information has shown the exact crystal packing with hexagonal symmetry for crystalline Gd<sub>2</sub>O(CO<sub>3</sub>)<sub>2</sub>·H<sub>2</sub>O sample.; (ii) These newly prepared Gd-containing particles showed the effective bimodal T<sub>1</sub>-positive and T<sub>2</sub>-negative contrast agents. The biodistribution studies indicated that the particles could circulate in the vessels and possibly metabolically excreted from organs after 12 h.; (iii) The Gd<sub>2</sub>O(CO<sub>3</sub>)<sub>2</sub>·H<sub>2</sub>O spherical particles potentially acted as multimodal particles because of readily surface engineering, which was normally limited in the inorganic Gd-related particles. We thus demonstrated that the Gd<sub>2</sub>O(CO<sub>3</sub>)<sub>2</sub>·H<sub>2</sub>O spheres as an ideal template to form hollow silica nanoshells and hollow silica@Fe<sub>3</sub>O<sub>4</sub> hybrid particles, which was reported for the first time.

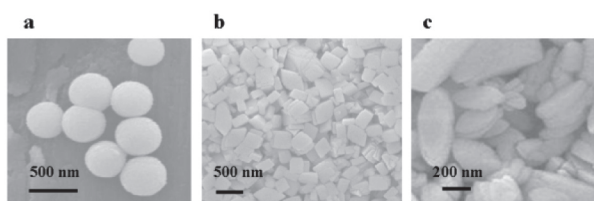


**Fig. 1:** SEM images showing (a) the spherical particles obtained from a ratio of  $[\text{urea}]/[\text{GdCl}_3 \cdot 6\text{H}_2\text{O}] = 4$  for a reaction of 4 h at 91 °C, (b) the rhombus-shaped particles obtained from a ratio of  $[\text{urea}]/[\text{GdCl}_3 \cdot 6\text{H}_2\text{O}] = 4$  for a reaction for 10 h at 91 °C, and (c) the rice-shaped mixtures obtained from a ratio of  $[\text{urea}]/[\text{GdCl}_3 \cdot 6\text{H}_2\text{O}] = 8$  for a reaction for 10 h at 91 °C

The  $\text{Gd}_2\text{O}(\text{CO}_3)_2 \cdot \text{H}_2\text{O}$  particles were synthesized by refluxing the aqueous solutions containing gadolinium salt and urea. Figure 1a shows the spherical particles obtained exclusively from a ratio of  $[\text{urea}]/[\text{GdCl}_3 \cdot 6\text{H}_2\text{O}] = 4$  for a reaction of 4 h at 91 °C. The spherical particles have an average diameter of  $478 \pm 70.8$  nm. With the same ratio of  $[\text{urea}]/[\text{GdCl}_3 \cdot 6\text{H}_2\text{O}] = 4$ , the reaction time was extended to 10 h resulting in at least 87% of the rhombus-like products accompanied by some rectangle-shaped particles (Fig.1b). The rhombus-shaped particles displayed the average size of 471.2 nm (height)  $\times$  198.9 nm (diameter). If the ratio of  $[\text{urea}]/[\text{GdCl}_3 \cdot 6\text{H}_2\text{O}]$  increased up to 8 by refluxing the solution for 10 h, polymorph structures including rice-shaped (61%), rectangle-shaped (23%) and other irregular (16%) particles were obtained. The rice-shaped particles with the average length of  $585.1 \pm 143.0$  nm and the diameter of  $214.7 \pm 53.0$  nm were produced under this experimental condition (Fig. 1c). FT-IR analysis was conducted for both sphere and rhombus samples and exhibited the identical spectrum. The absorbance band near  $\sim 3500$   $\text{cm}^{-1}$  could be attributed to O-H stretching in molecular  $\text{H}_2\text{O}$ . The three characteristic bands of  $\nu_{\text{as}}\text{O-C-O}$  (1539 and 1465  $\text{cm}^{-1}$ ),  $\pi\text{CO}_3^{2-}$  (860 and 848  $\text{cm}^{-1}$ ), and  $\delta\text{CO}_3^{2-}$  (729 and 721  $\text{cm}^{-1}$ ), provided the presence of carbonate. We have determined the  $\zeta$  potential of the sphere and rhombus samples to be +33 and +29 mV, respectively.

XRD measurements were performed to identify the resulting particles. Spherical particles showed no apparent peaks, indicating an amorphous structure. The rhombus-shaped particles were studied for XRD and the crystalline structure was observed, which is different from

the amorphous spheres. Interestingly, the rice-shaped mixtures exhibited the same pattern as the rhombus sample. The XRD patterns obtained from rhombus and rice-shaped particles are similar to gadolinium oxide carbonate hydrate ( $\text{Gd}_2\text{O}(\text{CO}_3)_2 \cdot \text{H}_2\text{O}$ , JCPDS no. 43-0604). Unfortunately, there is no unit cell and crystal symmetry information in the JCPDS file. Therefore, the high resolution synchrotron X-ray powder diffraction of the rhombus  $\text{Gd}_2\text{O}(\text{CO}_3)_2 \cdot \text{H}_2\text{O}$  sample was performed. We have indexed the synchrotron XRD pattern by both DICVOL and TREOR90 programs. Both results suggest that the rhombus  $\text{Gd}_2\text{O}(\text{CO}_3)_2 \cdot \text{H}_2\text{O}$  sample crystallizes in the hexagonal phase with a cell dimension of  $a = 10.2267$ ,  $c = 7.4178$ ,  $\text{vol.} = 671.8$ . The pattern can be fitted to the space group of  $\text{P6}_3/\text{m}$  (no. 176). No impurity crystalline phase was found in the diffraction pattern according to the Pawley refinement. Once again, a large amount of amorphous structures were detected and there exists 1 % less crystalline in the sphere particles, which is the same as that of the rhombus sample. This clearly suggests that these two samples have the exact crystal packing form. The temperature-dependent of XRD patterns provides the evidence for the structure conversion. The temperature was increased up to 700 °C and the samples were heated for 3 h for each calcined temperature in the air. For sphere particles, the  $\text{Gd}_2\text{O}_3$  crystalline appeared at 500 °C and completely converged at 600 °C. The rhombic  $\text{Gd}_2\text{O}(\text{CO}_3)_2 \cdot \text{H}_2\text{O}$  sample displayed the phase transition of  $\text{Gd}_2\text{O}_2\text{CO}_3$  at 400 °C and completely converted to  $\text{Gd}_2\text{O}_3$  (cube-like) at 700 °C.

We evaluated *in vitro* spin-lattice relaxation time ( $T_1$ ) weighted images and spin-spin relaxation time

( $T_2$ ) weighted images at 3T using 0.5% agarose gel for  $Gd_2O(CO_3)_2 \cdot H_2O$  (sphere and rhombus) and  $Gd_2O_3$  (sphere and cube-like) samples. A series of the different  $Gd^{3+}$  concentrations (0, 0.01, 0.05, 0.08, 0.1 mM) were investigated for the  $r_1$  and  $r_2$  relaxivities. The  $T_1$ -weighted MR signal of the  $Gd_2O(CO_3)_2 \cdot H_2O$  and  $Gd_2O_3$  became brightest at 0.05 mM with intensity increased to 120~140% and 170~180%, respectively. The concentration-dependent proton longitudinal relaxivities,  $r_1$ , were determined to be  $16.5 \text{ s}^{-1}\text{mM}^{-1}$  (spherical  $Gd_2O(CO_3)_2 \cdot H_2O$ ),  $22.2 \text{ s}^{-1}\text{mM}^{-1}$  (spherical  $Gd_2O_3$ ),  $13.1 \text{ s}^{-1}\text{mM}^{-1}$  (rhombic  $Gd_2O(CO_3)_2 \cdot H_2O$ ), and  $19.5 \text{ s}^{-1}\text{mM}^{-1}$  (cube-like  $Gd_2O_3$ ). On the  $T_2$ -weighted imaging sequences for both  $Gd_2O(CO_3)_2 \cdot H_2O$  and  $Gd_2O_3$ , the MR imaging intensity substantially darkened with increasing Gd concentration, which indicates that the  $T_2$ -lowering effect and signal decreases dominated at high concentration. The transverse  $r_2$  relaxivities were derived as  $210.7 \text{ s}^{-1}\text{mM}^{-1}$  (spherical  $Gd_2O(CO_3)_2 \cdot H_2O$ ),  $128.9 \text{ s}^{-1}\text{mM}^{-1}$  (spherical  $Gd_2O_3$ ),  $125.9 \text{ s}^{-1}\text{mM}^{-1}$  (rhombic  $Gd_2O(CO_3)_2 \cdot H_2O$  sample), and  $89.4 \text{ s}^{-1}\text{mM}^{-1}$  (cube-like  $Gd_2O_3$  sample). On the basis of the  $r_1$  and  $r_2$  relaxivities, the present  $Gd_2O(CO_3)_2 \cdot H_2O$  and  $Gd_2O_3$ , indeed, allowed to be applied as  $T_1$ -positive and  $T_2$ -negative contrast agents depend on the MR  $T_1$ -weighted and  $T_2$ -weighted sequences used. We have chosen the amorphous  $Gd_2O(CO_3)_2 \cdot H_2O$  sphere particles as an example to monitor the  $T_1$  contrast enhancement in mice. The dynamic contrast-enhanced MR imaging (DCE-MRI) technique was introduced to trace the imaging effect of the  $Gd_2O(CO_3)_2 \cdot H_2O$  spheres. The  $T_1$ -weighted images were recorded every 12 sec for a total of 12 min and 48 sec period. We injected the  $Gd_2O(CO_3)_2 \cdot H_2O$  spheres ( $0.3 \text{ mg kg}^{-1}$ ) at 6th repetition (at 61 sec) in the course of DCE-MRI imaging acquisition. In Fig. 2a, the DCE-MR imaging showed that the liver and kidney were apparently

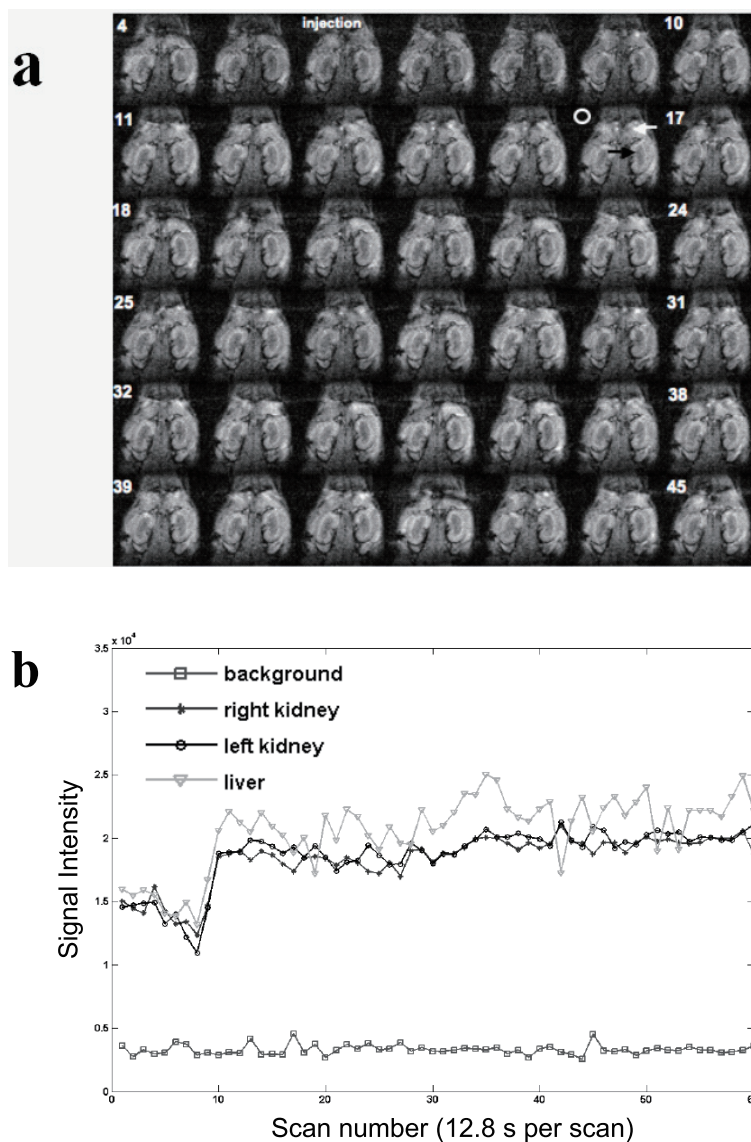


**Fig. 2:** The dynamic contrast-enhanced MR imaging (DCE-MRI) of the  $Gd_2O(CO_3)_2 \cdot H_2O$  (sphere-shaped particles). (a) The DCE-MR images from 4<sup>th</sup> to 45<sup>th</sup> repetition acquisitions that used gradient echo imaging sequence after injected particles ( $0.3 \text{ mg kg}^{-1}$ ) via retro-orbital plexus at 3T MR imaging system (white arrow: liver; black arrow: kidney; white circle: region of interest of background). (b) The signal profile in liver area (white arrow) and kidney area (black arrow) as compared with the background noise (white circle).

enhanced by  $Gd_2O(CO_3)_2 \cdot H_2O$  spheres starting from 10th (post 48 sec) repetition acquisition. Figure 2b displays that

the signal intensity of liver and kidney were measured as compared with the signal of the background noise marked as white circle throughout the acquisition. It is apparent that the signal contrast of liver and kidney were enhanced at 10th scan and remained brightness image up to 60th (post 10 min 48 sec) repetition acquisition. The evidence of the enhanced contrast in liver and kidney suggests that the amorphous  $\text{Gd}_2\text{O}(\text{CO}_3)_2 \cdot \text{H}_2\text{O}$  spheres could be introduced as an MR positive contrast agent.

Because of the presence of the  $-\text{OH}$  functional groups on the surface from FT-IR analysis and the positive surface charge from  $\zeta$  potential determination for the amorphous  $\text{Gd}_2\text{O}(\text{CO}_3)_2 \cdot \text{H}_2\text{O}$  spheres, both characteristics has made this material readily surface modification either by a hydrolysis and condensation of TEOS to form the silica shell or an electrostatic interaction using opposite charged species to yield various composition shells. Additionally, we have found that the resulting amorphous  $\text{Gd}_2\text{O}(\text{CO}_3)_2 \cdot \text{H}_2\text{O}$  spheres could be dissolved under acidic condition ( $\text{pH} \leq 2$ ). Hence, the hollow spheres with the diverse nanoshells could be obtained by using the designed surface modification, as seen in Fig. 3. Herein, the amorphous  $\text{Gd}_2\text{O}(\text{CO}_3)_2 \cdot \text{H}_2\text{O}$  spheres were demonstrated to serve as template particles by decorating the alkoxy silane for the silica hollow spheres.

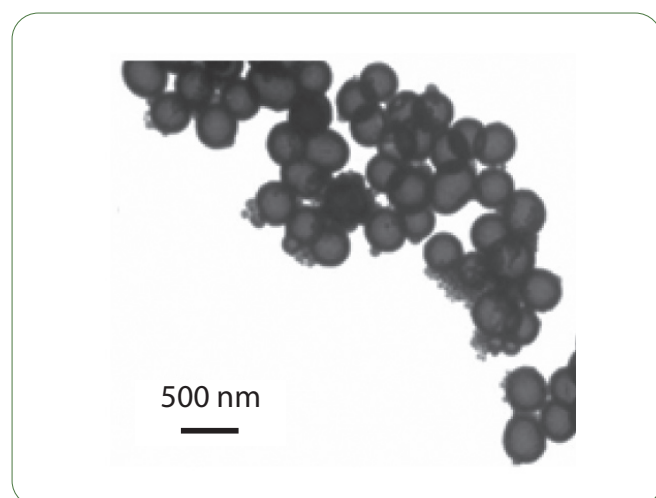


**Fig. 3:** TEM images of hollow silica spheres ( $\text{Gd}_2\text{O}(\text{CO}_3)_2 \cdot \text{H}_2\text{O}$ : 0.8 mg, ethanol: 3 mL, TEOS: 20  $\mu\text{L}$ , NaOH: 0.04 M).

In conclusion, the  $\text{Gd}_2\text{O}(\text{CO}_3)_2 \cdot \text{H}_2\text{O}$  colloidal particles have been prepared by a reflux of the mixture containing  $\text{GdCl}_3 \cdot 6\text{H}_2\text{O}$  and urea solution. In particular, the biocompatible amorphous  $\text{Gd}_2\text{O}(\text{CO}_3)_2 \cdot \text{H}_2\text{O}$  spheres have been demonstrated showing  $T_1$ -enhancing and  $T_2$ -lowering effects, which provide an alternative choice for an MRI contrast agent. Furthermore, the ready surface modification has led to the  $\text{Gd}_2\text{O}(\text{CO}_3)_2 \cdot \text{H}_2\text{O}$  spheres as an ideal template to form hollow nanoshells and hybrid composites. Based on the versatile combination strategy of the advantages of the surface engineering, MRI imaging and hollow structure shown by the  $\text{Gd}_2\text{O}(\text{CO}_3)_2 \cdot \text{H}_2\text{O}$  spheres hold the great potential in developing innovative composite materials and multifunctional biomaterials with imaging, targeting, delivery, and therapeutic capabilities in one. ◆

#### Experimental Station

01C2 Powder Diffraction

#### Publications

1. I. -F. Li, C. -H. Su, H. -S. Sheu, H. -C. Chiu, Y. -W. Lo, W. -T. Lin, J. -H. Chen, and C. -S. Yeh, *Adv. Funct. Mater.* **18**, 766 (2008).
2. C. -C. Huang, C. -H. Su, W. -M. Li, T. -Y. Liu, J. -H. Chen, and C. -S. Yeh, *Adv. Funct. Mater.* **19**, 249 (2009).

#### Contact E-mail

csyeh@mail.ncku.edu.tw